A Haptic Tele-Manipulation Environment for a Vibration-Driven Micromechatronic Device

Kostas Vlachos, Panagiotis Vartholomeos, and Evangelos Papadopoulos

Department of Mechanical Engineering,
National Technical University of Athens, 15780 Athens, Greece

***Abstract*—In this paper, a novel haptic tele-manipulation environment is presented. This includes an interface between a master haptic mechanism and a slave mechatronic mechanism for biomedical operations. The novelty stems from the fact that the environment's slave is a micromechatronic device driven by two inexpensive centripetal force vibration micromotors. The unique characteristics and challenges that arise during the haptic micromanipulation of the specific device are described and analyzed. The developed solutions are presented and discussed. The environment employs three input modes and two force control phases, which are described in detail. The haptic tele-manipulation environment is illustrated by several examples. These show that, while the interaction between the haptic mechanism and the vibration driven device is complicated, the micromanipulation of the device can be successful and appear to the operator as simple.**

***Index Terms*— Haptics, micro mechatronic device, micromanipulation, vibration-driven actuation.**

I. Introduction

In the last two decades, researchers worldwide focus in the micro or even nanoworld. Microsurgery or direct medical procedures on cells, biomechatronics, micromanufacturing, and microassembly, executed by micromechatronics devices are some of the fields of this research activity.

Usually, these devices are teleoperated microrobots. It is known that not only the visual but also the haptic feedback can be helpful for a successful teleoperated micromanipulation procedure, [1]. Therefore, some of the master manipulators are haptic devices, able to drive the microrobots and at the same time to transmit torques and forces to the operator.

A haptic teleoperation system, for use in microsurgery, was presented by Salcudean and Yan, [2], and by Salcudean, et al., [3]. The system consists of two magnetically levitated and kinematically identical wrists, acting as a macro-master and a micro-slave, and a conventional manipulator that transports them. A tele-nanorobotics system using an Atomic Force Microscope (AFM), as the nanorobot, has been proposed by Sitti and Hashimoto, [4]. The system provides a 1-dof force feedback device for haptic sensing, using a linear scaling approach. A microsurgical telerobot is presented, which consists of 6-dof parallel micromanipulator attached to a macro-motion industrial robot, and a 6-dof haptic master device, [5]. The system provides a disturbance observer to enhance the operator's perception.

A micro teleoperation system for micro tasks, such as assembly or manufacturing, was developed by Ando *et al.*, [6]. The haptic master is a 6-dof serial link mechanism, and the slave is a parallel link mechanism. Alternatively the Phantom, a commercial haptic interface, can be used as a master device, [7]. The Phantom is also used as a haptic master by Menciassi *et al.*, where a microinstrument for microsurgery or minimally invasive surgery was tested, [8]. Sitti *et al.* used the same haptic interface to teleoperate a piezoresistive atomic force microscope probe used as a slave manipulator and force sensor, [9]. A bio-micromanipulation system for biological objects such as embryos, cells or oocytes was presented in [10]. The system uses a Phantom to provide an augmented virtual haptic feedback during cell injection. A similar system for microinjection of embryonic stem cells into blastocysts is described in [11], although the system has no haptic feedback. The mechanical design of a haptic device integrated into a mobile nanohandling station is presented in [12]. The Delta haptic device was proposed as a nanomanipulator in [13]. The device is also interfaced to an AFM.

The scaling problem in macro-micro bilateral manipulation has been discussed by Colgate, where a condition for the robust stability of an operator/ bilateral manipulator/ environment system is derived using the structured singular value, [14]. Goldfarb addresses the issue of dynamic similarity and intensive property invariance in scaled bilateral manipulation, [15]. Using dimensional analysis methods yields a force-scaling factor that minimizes the intensive distortion of the environment. A force feedback control system for microassemply focusing on the issues of force transmission and control was presented, [16].

In this paper a novel haptic tele-manipulation environment is presented that includes an interface between a haptic mechanism and a micromechatronic device driven by two centripetal force actuators. Although the haptic master employed is a conventional haptic mechanism, it is the first time, to the knowledge of the authors, that a vibration driven micromechatronic device is considered as the slave. First, the

Manuscript received January 15, 2007. This work is co-funded by the European Social Fund (75%) and National Resources (25%)-(EPEAEK II)-PYTHAGORAS.

special characteristics and challenges that arise for the haptic micromanipulation due to the unique design of the micromechatronic device are described and analyzed. These unique characteristics concern not only the device's motion, but also the forces that appear during micromanipulation. Note here that the particular design of the micro platform (motion mechanism) rules out any consideration of designing a haptic master dedicated to the slave microrobot. The developed solutions are presented and discussed. The three input modes and two force phases employed are described in detail. Finally, the proposed haptic tele-manipulation environment is illustrated by several example applications. The examples show that, while the interaction between the haptic mechanism and the microrobot is complicated, the micromanipulation of the micro device can be successful and simple for the operator.

II. Characteristics and Limitations of the Haptic Tele-Manipulation System

The proposed haptic tele-manipulation environment employs an existing 5-dof haptic mechanism as the master and a 2-dof micromechatronic platform driven by two centripetal force actuators as the slave. A brief description of the master and slave is given next.

A. Master Haptic Device

The master device is the haptic mechanism shown in Fig. 1.

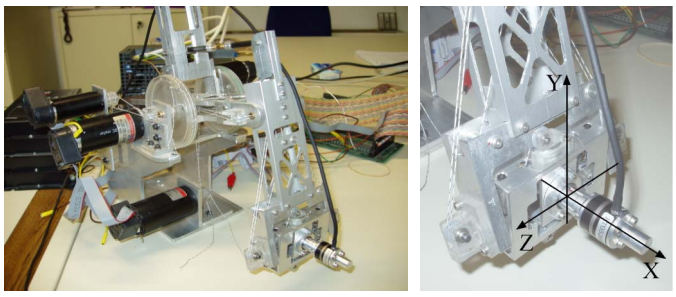

(a) (b)

Fig 1. (a) The haptic master. (b) Its force sensor equipped spherical joint.

It consists of a 2-dof, 5-bar linkage and a 3-dof spherical joint. All dof are active. To reduce mechanism moving mass and inertia, all actuators are placed at the base. The transmission system is implemented using tendon drives with capstans, [17]. Although this haptic device was not developed for micromanipulation, it is suitable since it has been designed optimally to exhibit maximum transparency, as seen from the operator side, [18].

Fig. 1(b) shows the macro world coordination system, i.e. the master haptic device system. The mechanism can translate in the X and Y axis by 10cm, rotate about the X axis by ±180º, and about the Y and Z axis by ±30º, maintaining at the same time its good functionality.

B. Slave Micromechatronic Platform

The slave device, shown in Fig 2a, is a micromechatronic platform employing two vibration microactuators. The motion mechanism is based on the interaction of centripetal forces generated by platform-mounted vibration micromotors and friction forces at the supports of the same platform. The concept was inspired by observing the motion of devices that vibrate, such as cellular phones or unbalanced washing machines, [19]. This is a novel, totally enclosed, design with application in the areas of microassembly, biomechatronics, microsurgery, etc.

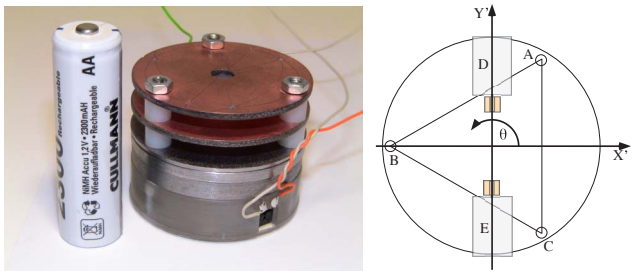

(a) (b)

Fig 2. The slave micromechatronic platform.

The platform can perform translational and rotational sliding with submicrometer positioning accuracy and velocities up to 1.5 mm/s. All the components of the mechanism, including its driving units, are of low cost and readily available. In Fig. 2b, the micro world coordination system is shown. The platform translates in the X axis and rotates about the Z axis by an angle θ.

C. Characteristics and Limitations of the Microplatform

The design and special characteristics of the slave micromechatronic platform (microrobot) lead to a number of challenges that need to be solved by the design of the tele-manipulation environment. These are presented next.

1. The slave microrobot is a mobile platform designed to perform tasks, like moving parts at the micro scale in cooperation with other similar microrobots, as for example during microassembly. The microrobot is not transported to its target by a macro robotic mechanism. Its translational sliding velocity is up to 1.5 mm/s.
2. The microplatform is equipped with two vibration microactuators, only.
3. The slave microplatform and the master haptic device are kinematical dissimilar. The first is a 5-dof robotic mechanism and the later is a 2-dof mobile platform.
4. It is impossible to analytically obtain the inverse kinematics of the nonlinear microrobot in real time.
5. The microrobot vibrates vertically when it reaches the 80% - 90% of the maximum theoretical velocity. The upper limit depends on the type of the ground.
6. Due to frictional forces, the micromechatronic platform stops sliding before the vibrating actuators stop.
7. Because of the vibrating nature of the microplatform actuation, the forces applied on the microtargets have the form of impacts.

D. Requirements for the Haptic Device

The above characteristics and limitations of the slave microrobot define the requirements for the master haptic device. Next, these requirements are presented.

1. The master haptic device has to drive the microplatform a) towards the microtarget, and b) during the micromanipulation. During the first phase we need more

velocity and less positioning accuracy, and in the second case the opposite.

2. To resolve the kinematical dissimilarity between the master and the slave, taking into account that an inverse kinematic relationship is unavailable in real time, a mapping from the master haptic device Cartesian space to the microrobot joint space has to be developed.
3. Since the mobile robot has two vibration microactuators, for submicrometer positioning accuracy, each actuator must be driven separately.
4. Furthermore, to rotate the micromechatronic platform without translation, the actuators must have rotational velocities with opposite directions. The master haptic device must also be able to realize this operation mode.
5. The force feedback mechanism should transfer the microforces of the microenvironment to the operator macroenvironment according to a suitable function. This function must handle not only smooth forces, but impact forces as well.

Next, the implementation of the above requirements to the haptic tele-manipulation environment is described.

III. The Tele-Manipulation Environment

The main elements of the haptic tele-manipulation system are the master haptic device and the slave micromechatronic platform. There is a bilateral communication between these devices.

The first communication channel, i.e. from the haptic mechanism to the microplatform, has the following inputs/outputs. PWM circuits drive the microplatform actuators. The input to the PWMs is the percentage (0-100%) of their duty cycle, and as a result the percentage of the microrobot actuator velocities. The output is the translation and rotation of the microrobot. Consequently the output of the master haptic device should be the percentage (0-100%) of the PWM duty cycle. The input to the haptic mechanism is obviously the command of the operator's hand.

The second communication channel, i.e. from the microrobot to the haptic mechanism, has as input the microforces sensed by the microrobot during manipulation. These forces are transmitted to the haptic device. The output of the communication channel is the force that the haptic device applies to the operator.

In order to realize the first communication channel from the haptic mechanism to the microplatform, the following three mutually exclusive input modes are defined.

A. Input Modes

The first is the *Macroscopic Mode* (MaM), the second is the *Macroscopic Rotation Mode* (MRM), and the third is the *Microscopic Mode* (MiM). Our goal in the first two input modes is to achieve coarse motion of the platform, while in the third mode it is to achieve fine micromanipulation.

1) The Macroscopic Mode

The master haptic manipulator uses this mode in order to drive the micromechatronic platform towards the microtarget. In this mode the positive/ negative translation of the master haptic mechanism end-effector in the X axis results in increase of the positive/negative rotational speed of *both* microrobot vibration microactuators and therefore results in microrobot translation along the X axis. To obtain a curved translation, a difference in the microactuator rotational velocities must be imposed. This is achieved by rotating the haptic device end-effector about the Y axis. A positive/ negative rotation about this axis results in an increase of the rotational speed of the first/ second microactuator.

As mentioned earlier, the device end-effector can translate in the X axis by 10 cm and rotate about the Y axis by about ±30°. Therefore the start point of the end-effector is at the middle of that distance, see Fig 3. A translation of the haptic device end-effector from start point "a" results in a percentage command of the microactuator speeds q according to,

$$q = -20(p-5) \quad [\%] \qquad (1)$$

where p [cm] is the haptic device end-effector position.

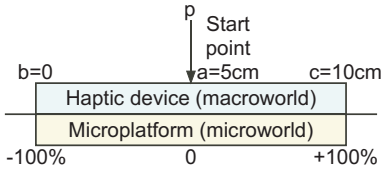

Fig 3. The MaM input scheme.

Additionally, for each degree of the end-effector rotation about the Y axis, the corresponding microactuator speed is increased by 1%.

2) The Macroscopic Rotation Mode

The master haptic manipulator uses this mode to rotate the microrobot without any translation. Pure rotation is convenient in order to change fast the direction of the microplatform translation. This can be achieved by rotating the microactuators in opposite speeds. To do this, the master operator translates the end-effector in the X axis resulting in an increase of the positive/ negative rotational speed of both microactuators, but this time in opposite direction.

3) The Microscopic Mode

The master haptic manipulator uses this mode during the micromanipulation. This mode is developed for fine motion of the microplatform assuming that it has reached the microtarget and it is ready for micromanipulation. Because of anisotropies in the behavior of the microplatform translation when both microactuators are functioning, see [19], for smooth and fine motion the microactuators have to function one at a time. To produce such a motion, the operator of the master device translates the end-effector in the positive or negative direction in the X axis indicating the rotation velocity and direction of the microactuators, and at the same time rotates the end-effector about the Y axis to indicate which microactuator should function.

Table I illustrates the above presented input modes. The "+"/ "–" symbols denote a positive/ negative rotational microactuator speed, the "↑" symbol denotes a microactuator speed increase, while "0" denotes that the corresponding microactuator is not influenced. During the MiM phase, "1" denotes that the corresponding microactuator is functioning,

"0" denotes that the corresponding microactuator is not functioning.

TABLE I
HAPTIC TELE-MANIPULATION ENVIRONMENT INPUT MODES

	MaM		MRM		MiM	
In X pos.	+	+	+	—	+	+
In X neg.	—	—	—	+	—	—
About Y pos.	↑	0	↑	0	1	0
About Y neg.	0	↑	0	↑	0	1
	Microactuator 1	Microactuator 2	Microactuator 1	Microactuator 2	Microactuator 1	Microactuator 2

In order to realize the second communication channel from the microrobot to the haptic mechanism, we define the following control phases.

B. Control Phases

Using the haptic device to control the micromechatronic platform, two control phases are identified. The first one is the *Macroscopic Control Phase*. During this phase the haptic mechanism operator drives the microplatform towards the microtarget. The second is the *Microscopic Control Phase*, in which the micromanipulation of the microtarget occurs. Next, both phases are presented in detail.

1) The Macroscopic Control Phase

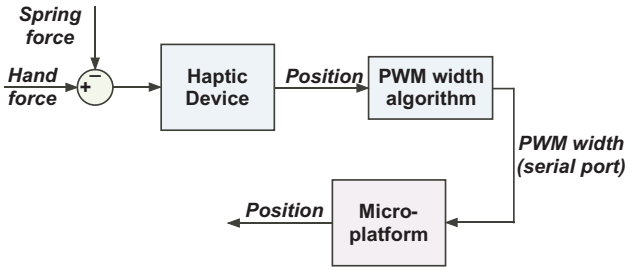

Fig. 4. The macro force loop (macroscopic control phase).

During this control phase, no micromanipulation forces exist, and therefore the haptic device does not apply forces to the operator. Instead, a spring force proportional to haptic end-effector translation is applied in order to indicate the increase in velocity, see Fig. 4. This is useful because the microrobot, after a certain velocity, starts to tip. Therefore, feedback of approaching this limit is provided to the operator. The applied spring force is described by,

$$f_{sp} = kp \qquad (2)$$

where p is the haptic device end-effector translation, see Fig. 3, and k is a variable spring constant. By experimentation, it was found that tipping occurs at about 80% of the maximum microactuator speed, depending on ground type or platform mass. To signal this limit, a spring constant three times harder is employed above the 80% of the maximum speed.

2) The Microscopic Control Phase

During this control phase, forces resulting from the micromanipulation are applied to the operator by the haptic device. As seen in Fig. 5, the microplatform following the operator commands comes to contact with the microenvironment, e.g. pushes a microobject. The produced force is measured and fed, according to a suitable scaling function, to the operator's hand from the haptic device.

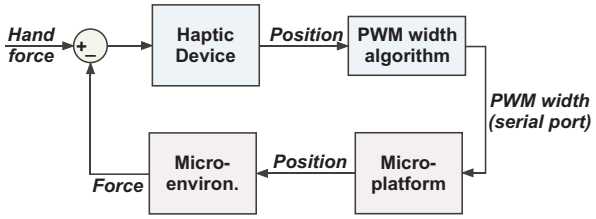

Fig 5. The micro force loop (microscopic control phase).

Because of the design of the microrobot, the generated forces have the form of impacts, [19]. Therefore, a simple forces magnification does not provide a useful haptic information, while it may be potentially dangerous for both the operator and the haptic device. To overcome this problem, we use filtering of the impact forces. This is a smooth signal, which is then magnified and applied to the operator. Here, an experimentally sound scale factor is 100.

IV. EXPERIMENTS

A. Experimental Setup

The experimental setup consists of three blocks, see Fig. 6. The first is the *Macro block*, where the operator translates the haptic device end-effector in the X axis and rotates it about the Y axis. The position and angle are captured by encoders attached on the haptic device actuators (Maxon dc motors), and transmitted to a PC/104 tower. This tower is the control unit, running the algorithm that translates the operator input into the microrobot input according to (1).

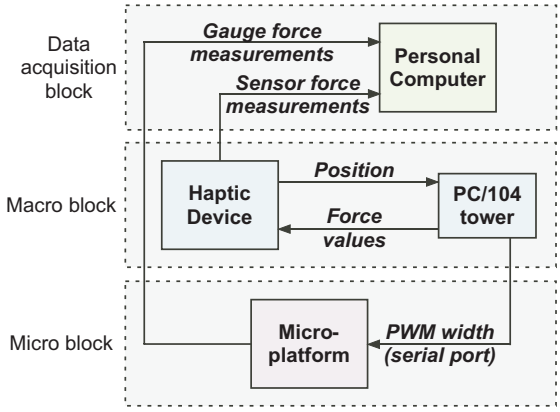

Fig 6. The experimental setup.

The *Micro block* consists of the microrobot, a 1 dof strain gauge force sensor attached to it, and the PWM circuits. The input to the PWMs is transmitted from the PC/104 tower through a serial port. If the microrobot micro manipulates a microobject, the strain gauge captures the produced microforces and transmits them to a PC in the *Data acquisition block*. From there, these forces are passed to the PC/104 tower, and after suitable scaling and smoothing, the necessary commands are send to the haptic device actuators by the PC/104 I/O card. The applied forces to the operator are measured by an ATI nano17 6-dof force sensor, attached on the haptic device end-effector. These measurements are also passed to the *Data acquisition block*.

In order to find the microplatform path during the experiments, we video-record the microplatform motion. The

video file is then processed by image processing routines of the *Image Processing Toolbox* of Matlab. To improve the results, we added white round marks on the top surface of the microrobot, see Fig. 7(a). Fig. 7(b) shows a schematic view of the top cover of the microrobot with the white marks, m_1, m_2, and m_3, and the platform center m_c. The image processing routines determine the coordinates of the three marks at each frame. Assuming these are placed on the three vertices of an isosceles triangle, we can calculate the angle θ according to (3), and the coordinates of the platform center, $m_{c,x}$, $m_{c,y}$, at each frame according to (4),

$$\theta = \arcsin\left(\frac{m_{1,y} - m_{3,y}}{\sqrt{(m_{1,x} - m_{3,x})^2 + (m_{1,y} - m_{3,y})^2}}\right) \quad (3)$$

$$\begin{aligned} m_{c,x} &= m_{1,x} + l_{m1c}\cos(30^\circ + \theta) \\ m_{c,y} &= m_{1,y} - l_{m1c}\sin(30^\circ + \theta) \end{aligned} \quad (4)$$

where $m_{i,x}$ and $m_{i,y}$, are the coordinates of mark m_i, and l_{m1c} is the distance between mark m_1 and the center m_c, according to,

$$l_{m1c} = \frac{\sqrt{(m_{1,x} - m_{2,x})^2 + (m_{1,y} - m_{2,y})^2}}{2\cos(30^\circ)} \quad (5)$$

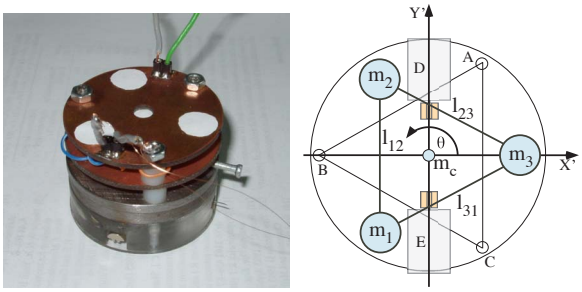

(a) (b)

Fig 7. (a) The microplatform with white marks. (b) Mark locations.

The output is the trajectory of the micromechatronic platform frame by frame. With a frame rate of 60 fps, a resolution of 1.7 pixels can be achieved. In this case, where a 115.2 × 92.16 mm surface is covered by a frame of 720 × 576 pixels, the resolution is 0.3 mm, which is acceptable during the macroscopic mode.

B. Experimental Results

We have executed five different experiments. The first four of them aimed at studying the behavior of the haptic tele-manipulation environment during the three different input modes. The last one examines the forces applied to the operator by the haptic device during a contact between the microrobot and a rigid obstacle.

1) MaM experiment

Two experiments are executed in the MaM input mode. In the first one, the master haptic device operator drives the microplatform in a straight line. The result is shown in Fig. 8.

The left plot shows the output of the image processing algorithm. The right plots are the x, y and θ coordinates of the microplatform geometric center. We can see from the third plot at the right side of Fig. 8 that the operator has to make several correctional moves by rotating the microrobot. This is expected since the same command to the microactuators results in different rotational velocities due to several platform anisotropies, see [19]. The haptic command was between 65 and 75% of the maximum velocity. In order to correct the translation, a ± 20% difference between the two microactuator speeds was initiated.

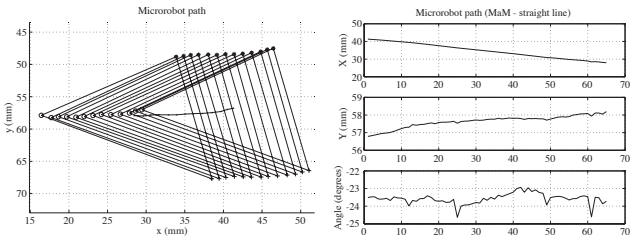

Fig 8. The microrobot path during a MaM experiment in straight line.

In the second experiment, the master haptic device operator drives the microrobot in a curved path, see Fig. 9. This is achieved by setting a difference of 25% between the two microactuator speeds, by rotating the haptic device end-effector for 25° about the Y axis.

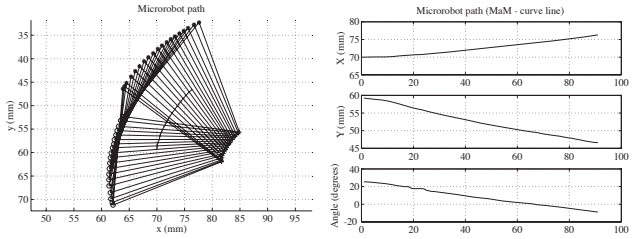

Fig 9. The microrobot path during a MaM experiment in curved line.

2) MRM experiment

In the MRM experiment we gave the same speed to the microactuators, but with opposite directions. The plus and minus arrows in Fig 10 show the direction change, which is also visible on the plot of the angle θ of the microrobot at the right side. We can see that a translation of 3-4 mm exists along with the desired pure rotation. The reason is that the microactuator speeds were not equal, although they had the same command. However, this can be adjusted.

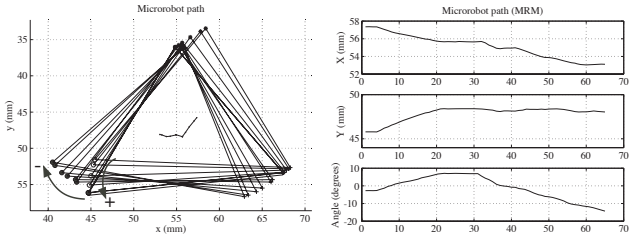

Fig 10. The microrobot path during a MRM experiment.

3) MiM experiment

The next experiment deals with the motion of the microplatform in the MiM mode. The best method to achieve a smooth trajectory and a fine resolution is to actuate the two microactuators one at a time. The result is shown in Fig. 11, where we can see the "slalom" motion of the platform.

Note here that in order to start the motion, the command to the microactuators should exceed 70-75% for a very short period, because of frictional forces. This problem can be

solved by a software routine, which when it is called initiates such a command for a very short period and then returns to 50% of the maximum velocity.

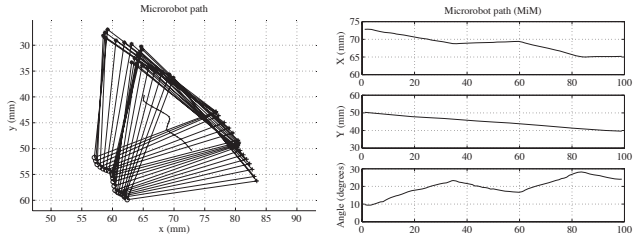

Fig 11. The microrobot path during a MiM experiment.

The experiments show that the operator should not decrease the command below of 45% of the maximum speed, because the microactuators stop due to friction. As before, to avoid platform tipping, the command should not exceed the 85-90%. The ideal operation space is between 60 and 85% depending on the input mode. These values depend on many environmental parameters, like the type and the situation of the ground or the mass of the platform. However, they can be easily determined.

4) Force experiment

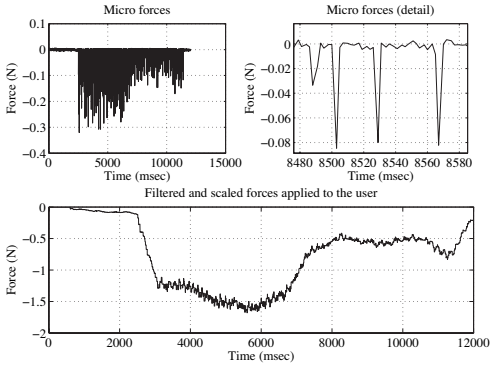

Fig 12. The impact forces applied to the operator with and without filtering.

This experiment studies the forces applied to the operator by the haptic device during a contact between the microrobot and a rigid obstacle. The experiment was conducted for 80 and 70% of the maximum microactuator velocities. Because of the high stiffness of the obstacle, the sensed forces have the form of impacts. Fig 12 shows these forces. The top right plot shows in detail the impacts. By smoothing the signal and using the scaling factor defined in Section III, the forces illustrated in the bottom plot of Fig. 12, are obtained.

V. CONCLUSIONS

In this paper, a novel haptic tele-manipulation environment is presented. This includes an interface between a master haptic mechanism and a slave mechatronic mechanism for biomedical operations. The novelty stems from the fact that the environment's slave is a micromechatronic device driven by two inexpensive centripetal force vibration micromotors. The unique characteristics and challenges that arise during the haptic micromanipulation of the specific device are described and analyzed. The developed solutions are presented and discussed. The environment employs three input modes and two force control phases, which are described in detail. The haptic tele-manipulation environment is illustrated by several examples. These show that, while the interaction between the haptic mechanism and the vibration driven device is complicated, the micromanipulation of the micromechatronic device can be successful and appear simple to the operator.

REFERENCES

[1] S. E. Salcudean, S. Ku, and G. Bell, "Performance measurement in scaled teleoperation for microsurgery," in *Proc. First Joint Conf. Computer Vision, Virtual Reality and Robotics in Medicine and Medial Robotics and Computer-Assisted Surgery (CVRMed-MRCA'97)*, 1997, Grenoble, France, pp. 789-798.

[2] S. E. Salcudean and J. Yan, "Towards a Force-Reflecting Motion-Scaling System for Microsurgery," in *Proc. IEEE Int. Conf. on Robotics and Automation (ICRA '94)*, 1994, San Diego, CA, USA, pp. 2296-2301.

[3] S. E. Salcudean, N. M. Wong, and R. L. Hollis, "Design and Control of a Force-Reflecting Teleoperation System with Magnetically Levitated Master and Wrist," *IEEE Trans. on Robotics and Automation*, Vol. 11, No. 6, December 1995, pp. 844-858.

[4] M. Sitti and H. Hashimoto, "Tele-Nanorobotics Using Atomic Force Microscope," in *Proc. IEEE/RSJ Int. Conf. on Intelligent Robots and Systems*, October 1998, Victoria, B.C., Canada, pp. 1739-1746.

[5] D. S. Kwon, K. Y. Woo, and H. S. Cho, "Haptic Control of the Master Hand Controller for a Microsurgical Telerobot System," in *Proc. IEEE Int. Conf. on Robotics and Automation (ICRA '99)*, May 1999, Detroit, Michigan, USA, pp. 1722-1727.

[6] N. Ando, M. Ohta, and H. Hashimoto, "Micro Teleoperation with Haptic Interface", in *Proc. of 2000 IEEE Int. Conf. on Industrial Electronics, Control and Instrumentation (IECON2000)*, October 2000, Nagoya, Japan, pp.13-18.

[7] T. Massie, and J. K. Salisbury, "The Phantom Haptic Interface: A Device for Probing Virtual Objects," in *Proc. ASME Winter Annual Meeting, Symposium on Haptic Interfaces for Virtual Environment and Teleoperator Systems*, Chicago, IL, November 1994, pp. 295-301.

[8] A. Menciassi, A. Eisinberg, M. C. Carrozza, and P. Dario, "Force Sensing Microinstrument for Measuring Tissue Properties and Pulse in Microsurgery," *IEEE/ASME Trans. on Mechatronics*, Vol. 8, No. 1, March 2003, pp. 10-17.

[9] M. Sitti, B. Aruk, H. Shintani, and H. Hashimoto, "Scaled Teleoperation System for Nano-Scale Interaction and Manipulation," *Advanced Robotics*, Vol. 17, No. 3, 2003, pp. 275-291.

[10] M. Ammi and A. Ferreira, "Realistic Visual and Haptic Rendering for Biological-Cell Injection," in *Proc. IEEE Int. Conf. on Robotics and Automation (ICRA '05)*, April 2005, Barcelona, Spain, pp. 930-935.

[11] L. Mattos, E. Grant, and R. Thresher, "Semi-Automated Blastocyst Microinjection," in *Proc. IEEE Int. Conf. on Robotics and Automation (ICRA '06)*, May 2006, Orlando, Florida, USA, pp. 1780-1785.

[12] A. Kortschack, A. Shirinov, T. Trueper, and S. Fatikow, "Development of Mobile Versatile Nanohandling Microrobots: Design, Driving Principles, Haptic Control," *Robotica*, v. 23, n. 4, July 2005, pp 419-434.

[13] S. Grange *et al.*, "The Delta Haptic Device as a Nanomanipulator," in *Proc. SPIE Microrobotics & Microassembly II*, v. 4568, 2001, pp. 100-111.

[14] J. E. Colgate, "Power and Impedance Scaling in Bilateral Manipulation," in *Proc. IEEE Int. Conf. on Robotics and Automation (ICRA '91)*, April 1991, Sacramento, CA, USA, pp. 2292-2297.

[15] M. Goldfarb, "Dimensional Analysis and Selective Distortion in Scaled Bilateral Telemanipulation," in *Proc. IEEE Int. Conf. on Robotics & Automation,* May 1998, Leuven, Belgium, pp. 1609-1614.

[16] Z. Lu *et al.*, "A Force-Feedback Control System for Micro-Assemply," in *Journal of Micromechanics and Microengineering*, Vol. 16, 2006, pp. 1861-1868.

[17] K. Vlachos, E. Papadopoulos, and D. Mitropoulos, "Design and Implementation of a Haptic Device for Urological Operations," *IEEE Trans. on Robotics & Aut.*, v. 19, no. 5, Oct. 2003, pp. 801-809.

[18] K. Vlachos and E. Papadopoulos, "Transparency Maximization Methodology for Haptic Devices," *IEEE/ASME Trans. on Mechatronics*, Vol. 11, No. 3, June 2006, pp. 249-255.

[19] P. Vartholomeos and E. Papadopoulos, "Analysis, Design and Control of a Planar Micro-robot Driven by Two Centripetal-Force Actuators," in *Proc. IEEE Int. Conf. on Robotics and Automation (ICRA '06)*, May 2006, Orlando, FL, USA, pp. 649-654.